Head-Ballistocardiography Morphology From Smart Eyewear for Cardiovascular Fitness and Recovery

Sarah Solbiati[1], Federica Mozzini[1], Cornelia Dancs[1], Enrico Gianluca Caiani[1,2]

[1]Politecnico di Milano, Electronics, Information and Bioengineering Dpt., Milan, Italy
[2]IRCCS Istituto Auxologico Italiano, Milan, Italy

Abstract

Smart eyewear can unobtrusively acquire head ballistocardiography (H-BCG), but prior work has mainly focused on heartbeat detection and heart rate (HR) estimation. This study investigates whether H-BCG morphological indices are sensitive to respiratory maneuvers and post-exercise recovery. Thirty healthy volunteers completed a static protocol and ten a dynamic exercise-recovery protocol, with simultaneous ECG and smart eyewear H-BCG recording. Beat-by-beat H-BCG beat were identified and amplitude and slope descriptors were extracted. Morphological descriptors varied with physiological condition, peaking during full-lung apnoea, while in the dynamic protocol amplitude and slope features increased after exercise and progressively declined during recovery, mirroring HR. Smart eyewear H-BCG morphology may thus provide candidate biomarkers of exercise-related cardiovascular recovery.

1. Introduction

Cardiorespiratory fitness is a strong marker of cardiovascular health, but reference-standard assessment by cardiopulmonary exercise testing is resource-intensive and difficult to deploy outside the laboratory [1–3]. This has driven growing interest in wearables for longitudinal, real-world cardiovascular monitoring. Recent work has shown that cardio-mechanical signals such as seismocardiography and ballistocardiography (BCG) can provide information beyond heart rate (HR), including markers related to stroke volume, cardiac output, and contractility, supporting their potential for unobtrusive cardiovascular monitoring [4-9].

Among these modalities, head-ballistocardiography (H-BCG) appears particularly attractive for everyday sensing, as subtle cardiac-induced head motions can be captured non- cardiac-induced head motions can be captured by 6-axis inertial sensors already embedded in head-worn wearables. BCG reflects the body's recoil to pulsatile blood acceleration during the cardiac cycle. When the sensor is rigidly coupled to the head, H-BCG reaction forces generated by blood acceleration and vascular dynamics, producing subtle motions of ~10 mG, corresponding to a ~5 mm displacement [10]. Although seismocardiography is more established for assessing cardiac mechanics and fitness [1], head-worn sensing may better support repeated and opportunistic monitoring without additional skin-contact sensors. Smart eyewear is especially promising in this respect: it offers stable coupling to the head, requires no direct skin contact, and it is compatible with continuous, real-world monitoring. Prior smart eyewear H-BCG studies have mainly focused on HR estimation [11,12], identifying the head–foot acceleration and roll rotation components as the most informative axes [12]. However, H-BCG waveform morphology remains underexplored and may provide cardiovascular information complementary to HR. Inferring such information with ECG-free approaches is key for fully self-contained smart eyewear monitoring. In this study, we move beyond conventional HR estimation to investigate how smart eyewear-derived H-BCG morphological indices vary across rest, breathing maneuvers, and post-exercise recovery.

2. Methods

2.1. Study population and design

Data were collected during two experimental protocols, referred to as "Static" (30 volunteers, 15 males and 15 females, age: 29.6±6.8 years) and "Dynamic" (10 volunteers, 5 males, 5F, age: 30.5.6±8.4 years), approved by the Ethics Committee of Politecnico di Milano (opinion n. 33/23 and opinion n. 20/24, respectively). All participants provided written informed consent.

The Static protocol comprised spontaneous breathing, paced breathing at four respiratory rates (4-s, 6-s, 8-s and 10-s respiratory cycles), and full- and empty-lung apnoea. The Dynamic protocol included a 3-min seated baseline, 15 min of submaximal cycling, and 15 min of treadmill exercise from slow walking to submaximal running, each followed by a 5-min seated recovery. In both protocols, single-lead ECG (1024 Hz, EcgMove4, Movisens GmbH) was acquired as reference, together with 3-axis accelerometer and gyroscope signals (100 Hz) obtained by prototype smart eyewear [13] (EssilorLuxottica, Milan, Italy), providing the H-BCG signals.

2.2. Signals processing

The ECG signals were band-pass filtered (0.5–30 Hz), and R peaks were identified using the Pan-Tompkins algorithm [14]. The acceleration and rotation signals were band-pass filtered (5–25 Hz) to attenuate the respiratory component, and motion-corrupted windows were excluded through a z-score-based outlier procedure.

H-BCG systolic complexes were detected using an ECG-free approach to enable a self-contained smart-eyewear framework. The Hilbert transform was used to estimate the local cardiac periodicity without relying on individual waveform extrema. The minimum J-peak distance was adaptively set to half the average J–J interval, preventing multiple detections per cardiac cycle while allowing beat-to-beat variability. For each axis, in each 11-s window, a systolic complex template was extracted and cross-correlated with the signal to identify candidate J peaks [15]. As H-BCG projection may vary with individual head mechanics or eyewear fit, the optimal axis was selected each time based on the lowest beat-to-beat interval fitting error [15], and used exclusively for HR estimation. The head-foot (H-F) acceleration and the Roll angular-velocity axes consistently emerged as the best-performing channels, in agreement with previous studies [12]. As they represent distinct linear and rotational components of cardiac-induced head motion, their morphology, magnitude, and units were interpreted separately. Accordingly, subsequent morphology analysis was focused on the H-F and Roll channels. For each subject, detected beats were extracted and aligned using dynamic time warping [16] to generate a representative template, identify morphological labels (I, J, K, and L), and derive amplitude (A_{IJ}, A_{JK}) and slope-based (S_{IJ}, S_{JK}) descriptors (Figure 1).

2.3. Statistical analysis

J-peak identification feasibility was quantified, and agreement between H-BCG- and ECG-derived HR was assessed by Bland–Altman analysis using median HR values from corresponding 11-s windows.

Experimental phase-related differences were assessed (Friedman, $p<0.05$, post-hoc Wilcoxon signed-rank test with Bonferroni correction). To describe cardiovascular dynamics, morphology-derived indices were also tracked during recovery using median values from consecutive 11-s windows across rest and post-exercise recovery.

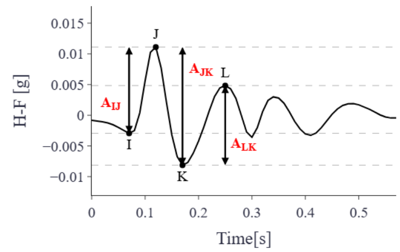

Figure 1. Example of a H-BCG cardiac beat and the identified fiducial points.

3. Results

J-peak detection feasibility was high across all analysed phases. In the Static Protocol, median feasibility ranged from 89.8% [85.7–93.9] during paced breathing to 100% [94.9–100] and 100% [95.2–100] during full- and empty-lung apnoea, respectively. In the Dynamic Protocol, it ranged from 83% [72.2–88.1] to 86.6% [78.8–91.4] across post-exercise recovery phases.

Bland–Altman analysis (Figure 2) confirmed good agreement between HR values derived from H-BCG and ECG in all static phases, with non-significant small bias in every condition, and wider limits of agreement observed in the Dynamic Protocol.

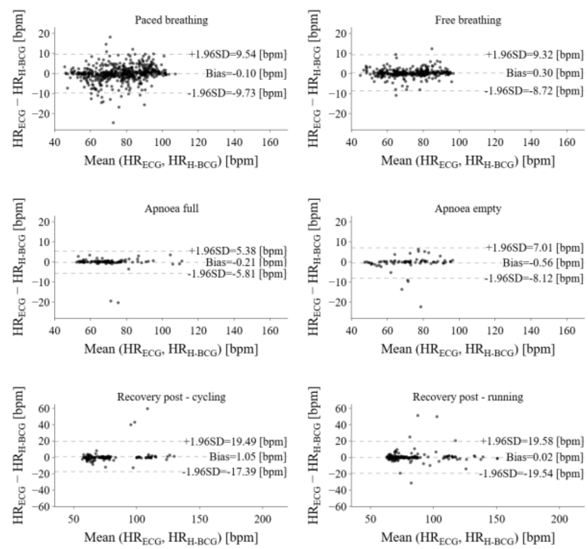

Figure 2. Bland Altman showing the comparison between ECG-derived HR and H-BCG-derived HR.

Morphological H-BCG descriptors varied across phases and showed different sensitivities depending on the considered axis. In the Static Protocol (Table 1), the morphological features of the Roll axis remained relatively stable across breathing conditions, whereas clearer modulation was observed along the H-F axis, with A_{JI}, A_{JK}, S_{JI}, and S_{JK} peaking during full-lung apnoea. In the Dynamic Protocol, a trend of increased amplitude and slope indices from baseline to recovery was observed, with the highest values generally observed after walking/running; however, significant differences were limited to A_{LK} and S_{JI} on the Roll axis (Table 2).

Table 1. Morphological parameters computed along the H-BCG H-F axis in the Static Protocol phases. *: vs free breathing; †: vs paced breathing; ‡: vs apnoea full.

	Free breathing	Paced breathing	Apnoea full	Apnoea empty
A_{IJ} (mg)	6.3 [4.7;8.6]	7.2 [6.0; 10.1] *	9.0 [7.2; 12.6] *,†	6.0 [4.4; 8.8] †,‡
A_{JK} (mg)	5.9 [4.6;7.7]	7.3 [6.2;9.8] *	9.8 [8.0; 12.5] *,†	5.8 [4.8; 7.9] †,‡
A_{KL} (mg)	3.2 [1.8;4.2]	4.7 [3.5;6.1] *	5.1 [3.9;6.8] *	4.5 [2.7;5.7]
S_{IJ}	0.16 [0.10;0.22]	0.19 [0.14; 0.27]	0.27 [0.18;0.36] *,†	0.15 [0.09; 0.22] †,‡
S_{JK}	0.13 [0.10; 0.15]	0.13 [0.11; 0.17]	0.19 [0.14; 0.28] *,†	0.11 [0.08; 0.15] ‡

Table 2. Morphological parameters computed along the H-BCG Roll axis in the Dynamic Protocol phases. *: vs baseline.

	Baseline	Recovery post-cycling	Recovery post-walk/run
A_{IJ} (rpm)	0.54 [0.53;0.72]	0.93 [0.75;1.11]	1.01 [0.73;1.46]
A_{JK} (rpm)	0.79 [0.71;0.94]	1.50 [1.17;1.95]	1.55 [1.13;2.34]
A_{KL} (rpm)	0.68 [0.42;0.78]	1.06 [0.41;1.25]	0.93 [0.63;1.55] *
S_{IJ}	11.26 [9.63;15.88]	13.20 [12.69;25.39]	16.53 [14.04;37.57] *
S_{JK}	15.70 [14.30;18.99]	46.42 [27.67;54.07]	51.64 [26.40;56.00]

Figure 3 shows the % changes in A_{JI} relative to the baseline during the 5-min recovery period following submaximal treadmill exercise. Interestingly, A_{IJ} was elevated immediately after exercise and then progressively declined toward baseline, mirroring the corresponding decrease in HR.

4. Discussion

This study extends smart eyewear H-BCG analysis beyond conventional heartbeat detection and HR estimation, showing that morphology-derived descriptors could capture physiologically meaningful changes across respiratory manoeuvres and during post-exercise recovery.

The results are consistent with previous H-BCG studies, not limited to smart eyewear, identifying the H-F acceleration and Roll angular-velocity as the most informative axes for cardiac-related head motion [12]. Additionally, the improved ECG-free H-BCG beat detection method allowed to achieve markedly higher feasibility than previous approaches [12], increasing to 100 [94.9;100]% during full-lung apnoea, 100 [95.2;100]% during empty-lung apnoea, 89.8 [85.7;93.9]% during paced breathing, and from 73 [69;85]% to 97.2 [93.8;98]% during free breathing [12]. This improvement was paralleled by acceptable HR estimation agreement with ECG, especially during more still phases such as apnoea and free or controlled breathing. Interestingly, H-F amplitude and slope indices were higher during full- than empty-lung apnoea. Despite absent airflow in both conditions, different lung volumes may alter cardio-mechanical morphology through changes in intrathoracic pressure, cardiac loading, and heart position, possibly together with autonomic modulation reflected by HR [17].

The main finding is that morphology-derived H-BCG indices showed coherent post-exercise recovery trends. To the best of our knowledge, this is the first demonstration that amplitude- and slope-based H-BCG indices extracted from smart eyewear are sensitive to recovery dynamics in parallel with HR. Their post-exercise increase and progressive decline may reflect normalization of cardiac ejection dynamics and central hemodynamic loading. In conventional BCG, Amplitude and slope descriptors have been associated with ventricular ejection, stroke volume, cardiac output, and contractility [1]. H-F and Roll axes provide complementary but physically distinct representations of cardiac-induced head motion, capturing different components of the cardiovascular mechanical response. Future studies should investigate their specific physiological meaning and their contribution to recovery and fitness assessment. These results pave the way to potential scaling up and translational utilization, due to large diffusion of glasses in a large part of the population [18], potentially enabling more advanced cardiovascular monitoring without the need for additional sensors.

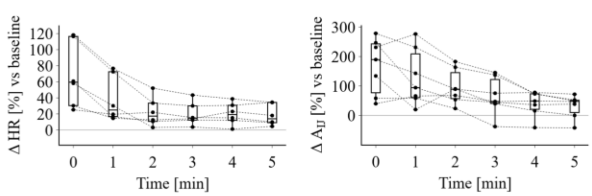

Figure 3. Trend of recovery of the HR and the A_{IJ} after the submaximal treadmill exercise.

In a scenario of opportunistic measurements [19,20], smart eyewear may offer unobtrusive digital biomarkers of cardiovascular fitness and recovery.

4. Conclusions

The analysis of H-BCG morphology extends cardio-mechanical sensing beyond HR estimation. Morphological descriptors changed across respiratory conditions and tracked post-exercise recovery, supporting the potential of smart eyewear H-BCG as an unobtrusive source of digital biomarkers of cardiovascular fitness and recovery.

Acknowledgments

This work was carried out in the EssilorLuxottica Smart Eyewear Lab, a Joint Research Center between EssilorLuxottica and Politecnico di Milano.

References

[1] S. E. Schmidt, M. T. Hansen, D. S. Karbing, K. Sørensen, M. K. Poulsen, T. Rømer, J. J. Struijk, P. Søgaard, and J. W. Helge, "Estimation of cardiorespiratory fitness in healthy using seismocardiography," *npj Cardiovasc. Health*, vol. 2, no. 1, Art. no. 16, 2025.

[2] M. P. Harber, J. Myers, A. R. Bonikowske, A. Muntaner-Mas, P. Molina-Garcia, R. Arena, and F. B. Ortega, "Assessing cardiorespiratory fitness in clinical and community settings: Lessons and advancements in the 100th year anniversary of VO2max," *Prog. Cardiovasc. Dis.*, vol. 83, pp. 36–42, Mar. 2024.

[3] A. Dosis, A. B. Syversen, M. R. Kowal, D. Grant, J. Tiernan, D. Wong, and D. G. Jayne, "Exploiting unsupervised free-living data for cardiorespiratory fitness estimation: Systematic review and meta-analysis," *JMIR Mhealth Uhealth*, vol. 14, no. 1, Art. no. e69996, Jan. 2026.

[4] I. Sadek, J. Biswas, and B. Abdulrazak, "Ballistocardiogram signal processing: a review," *Health Inf. Sci. Syst.*, vol. 7, no. 1, Art. no. 10, May 2019.

[5] G. Guidoboni, L. Sala, M. Enayati, R. Sacco, M. Szopos, J. Keller, M. Popescu, L. Despins, V. H. Huxley, and M. Skubic, "Cardiovascular function and ballistocardiogram: A relationship interpreted via mathematical modeling," *IEEE Trans. Biomed. Eng.*, vol. 66, no. 10, pp. 2906–2917, Oct. 2019.

[6] H. Ashouri, L. Orlandic, and O. T. Inan, "Unobtrusive estimation of cardiac contractility and stroke volume changes using ballistocardiogram measurements on a high bandwidth force plate," *Sensors*, vol. 16, no. 6, Art. no. 787, May 2016.

[7] J. N. Svensøy, E. Alonso, A. Elola, et al., "Cardiac output estimation using ballistocardiography: a feasibility study in healthy subjects," *Sci. Rep.*, vol. 14, Art. no. 1671, Jan. 2024.

[8] M. Etemadi and O. T. Inan, "Wearable ballistocardiogram and seismocardiogram systems for health and performance," *J. Appl. Physiol.*, vol. 124, no. 2, pp. 452–461, Feb. 2018.

[9] V. G. Ganti, A. H. Gazi, S. An, et al., "Wearable seismocardiography-based assessment of stroke volume in congenital heart disease," *J. Am. Heart Assoc.*, vol. 11, no. 18, Art. no. e026067, Sep. 2022.

[10] G. Balakrishnan, F. Durand, and J. Guttag, "Detecting pulse from head motions in video," in *Proc. IEEE Conf. Comput. Vis. Pattern Recognit. (CVPR)*, pp. 3430–3437, 2013.

[11] S. Solbiati, F. Mozzini, J. Sahler, P. Gil, B. Amir, N. Antonello, D. Trojaniello, and E. G. Caiani, "Estimating heart rate from inertial sensors embedded in smart eyewear: A validation study," *Sensors*, vol. 25, no. 15, Art. no. 4531, Jul. 2025.

[12] S. Solbiati, S. Charkas, F. Mozzini, A. L. Mauro, S. Bernasconi, A. Angelucci, A. Aliverti, D. Trojaniello, and E. G. Caiani, "Comparison of ECG-free algorithms for heart rate computation from head-BCG signals obtained with smart eyewear," in *2024 IEEE Int. Conf. Metrol. eXtended Reality, Artif. Intell. Neural Eng. (MetroXRAINE)*, pp. 213–218, Oct. 2024.

[13] I. Crupi, A. Scandelli, A. Giudici, G. Gervasoni, D. Trojaniello, and F. Villa, "Multi-Sensor Smart Eyewear for Biomarkers Acquisition," *IEEE Sens. J.*, vol. 25, pp. 40565–40574, Nov. 2025.

[14] J. Pan and W. J. Tompkins, "A real-time QRS detection algorithm," *IEEE Trans. Biomed. Eng.*, vol. BME-32, no. 3, pp. 230–236, Mar. 1985.

[15] F. Landreani, A. Faini, A. Martin-Yebra, M. Morri, G. Parati, and E. G. Caiani, "Assessment of ultra-short heart variability indices derived by smartphone accelerometers for stress detection," *Sensors*, vol. 19, no. 17, Art. no. 3729, Aug. 2019.

[16] E. G. Caiani, A. Porta, G. Baselli, M. Turiel, S. Muzzupappa, M. Pagani, A. Malliani, and S. Cerutti, "Analysis of cardiac left-ventricular volume based on time warping averaging," *Med. Biol. Eng. Comput.*, vol. 40, no. 2, pp. 225–233, Mar. 2002.

[17] S. Ahdy, T. Hassan, B. Rahman, R. H. Sandler, and H. A. Mansy, "SCG variability and spectral energy distribution during normal breathing and breath hold at different lung volumes and airway pressures," Sci. Rep., vol. 14, Art. no. 17904, 2024.

[18] J. A. Harvey, S. F. Chastin, and D. A. Skelton, "How sedentary are older people? A systematic review of the amount of sedentary behavior," *J. Aging Phys. Act.*, vol. 23, pp. 471–487, 2015.

[19] H. Xie, L. Yang, B. Jiang, Z. Huang, and Y. Lin, "State-of-the-art wearable sensors for cardiovascular health: A review," *npj Cardiovasc. Health*, vol. 2, Art. no. 53, 2025.

[20] A. Jamieson, T. J. A. Chico, S. Jones, *et al.*, "A guide to consumer-grade wearables in cardiovascular clinical care and population health for non-experts," *npj Cardiovasc. Health*, vol. 2, Art. no. 44, 2025.

Address for correspondence:

Enrico Gianluca Caiani
Piazza L. da Vinci 32
20133 Milano - ITALY
enrico.caiani@polimi.it